Nuclear Materials and Energy 15 (2018) 115–121

Contents lists available at ScienceDirect

Nuclear Materials and Energy

journal homepage: www.elsevier.com/locate/nme

Cavity evolution and hardness changes in a 15Cr-ODS ferritic steel by post He-implantation annealing

Peng Song[a,*], Kiyohiro Yabuuchi[b], Akihiko Kimura[b]

[a] Graduate School of Energy Science, Kyoto University, Yoshida-honmachi, Sakyou-ku, Kyoto 606-8501, Japan
[b] Institute of Advanced Energy, Kyoto University, Gokasho, Uji, Kyoto 611-0011, Japan

ARTICLE INFO

Keywords:
Cavity evolution
Nanoindentation hardness
ODS steel
He implantation
Annealing

ABSTRACT

15Cr-ODS ferritic steel was implanted with 3500 appm He (0.2 dpa) at 300, 550 and 700 °C. The post-implantation annealing (PIA) at 800 °C/100 h was conducted on the specimen implanted at 300 °C. Nanoindentation (NI) tests were carried out to investigate the temperature dependent hardening, and transmission electron microscopy (TEM) observation was performed to characterize the cavity evolution. A limited hardening was found in the as-implanted ODS specimens at all implantation temperatures, which tended to reduce with increasing the temperature. The PIA caused no further hardening, while TEM images revealed that there was an evident change in the cavity distribution morphology. The cavity diameter increased from 2.5 ± 0.4 nm to 5.0 ± 1.7 nm and the corresponding number density decreased from $(22.2 \pm 1.6) \times 10^{22}\ m^{-3}$ to $(6.7 \pm 0.5) \times 10^{22}\ m^{-3}$ before and after the PIA. The negligible hardness changes induced by the PIA were interpreted in terms of the Orowan-type dislocation barrier model with the corresponding barrier strength factor of cavities to be less than 0.1.

1. Introduction

Oxide dispersion strengthened (ODS) steels have been considered as a candidate structural material of first wall/blanket for future fusion reactors because of their outstanding mechanical properties, especially high-temperature strength [1,2], and acceptable corrosion resistance against coolants [1], as well as excellent radiation tolerance such as low swelling and hardening [2,3]. In the fusion structural material, numerous helium (He) atoms are produced by (n, α) nuclear reactions. Moreover, the formation of He-Vacancy (He-V) clusters, involving nanosized He bubbles, cavities and large voids, may lead to swelling, hardening, embrittlement and reduction in creep properties [4].

In the conventional ferritic/martensitic (F/M) steels, He-induced hardening is still a matter of discussion. Jung et al. investigated the effect of the implanted He on tensile properties of 9Cr-martensitic steels (EM10 and T91) using an ion accelerator at temperatures from 150 °C to 550 °C with He concentrations between 1250 and 5000 appm at 0.2 and 0.8 dpa, respectively [5]. Based on the dependence of irradiation hardening on He concentration and dpa, they attributed the hardening to He bubbles without TEM examinations [5]. Henry et al. [6] performed TEM examinations and SANS analysis for the same steels as those in Ref. [5] implanted with 5000 appm He. Indeed, they concluded again that the evident hardening was attributed to He bubbles at the implantation temperatures between 250 and 550 °C, although no He bubbles but dot shaped small defect clusters, probably dislocation loops, were observed by TEM in the steel implanted with 5000 ppm He at 250 °C. Additionally, they mentioned that the barrier hardening model with a strength factor of 0.4 gave an insufficient hardening by small defect clusters. Farrell et al. [7] compared the tensile properties of F/M steels irradiated in HFIR and LANSCE spanning the dose range 0.01–24 dpa up to about 1000 appm He. As a result, there was no sign of a large hardening contribution attributable to the presence of He at the irradiation temperatures below 160 °C. Furthermore, Henry et al. [8] reported on tensile properties of 9Cr-1Mo (EM10) tempered martensitic steel irradiated in spallation conditions (133–301 °C, 4–11 dpa, 150–890 appm He, 1270–4800 appm H) and after the irradiation with fission neutrons in OSIRIS reactor (325 °C, ~1–9.3 dpa) that the amount of irradiation hardening showed a similar trend of dose dependence. Dai et al. [9] investigated the dpa dependence of irradiation hardening of T91 irradiated at below 300 °C in SINQ Target-3, and reported that the dpa dependence of hardening was changed over 5.9 dpa (He = 390 appm) above which He bubbles contributed to an additional hardening. More recently, Dai et al. reported that an evident hardening ($\Delta HV = \sim 80\ kg/mm^2$) was left in the post-irradiation annealed (600 °C/2 h) F/M steels after the irradiation in SINQ (1175 appm/11.3 dpa), which was attributed to the contribution of He

* Corresponding author.
E-mail address: p-song@iae.kyoto-u.ac.jp (P. Song).

https://doi.org/10.1016/j.nme.2018.03.006
Received 9 January 2018; Received in revised form 11 March 2018; Accepted 12 March 2018
Available online 21 March 2018

bubbles [10].

As for the ODS F/M steels, the ODS F/M steel with He ion implantation (3360 appm/0.84 dpa) also presented a temperature dependent hardening behavior: declining from ~15% at 100 °C to ~3.5% at 500 °C [11], which might be accompanied by cavity evolution [12]. Nevertheless, some discrepancies still exist for the He induced hardening in ODS F/M steels. Roldán et al. reported that the implantation of about 750 appm He brought about a 21% hardening in Eurofer ODS at 70 °C [13], while at 30 °C/9 at.% He/3 dpa, a 31% hardening was produced in the same ODS steel [14]. At such low temperatures, it is difficult to separate the pure hardening contribution of He bubbles from those of fine defect clusters or dislocation loops.

Post-implantation annealing (PIA) may be an effective way to distinguish the contributions of dislocation loops and He-V clusters, and possibly lead to an assessment of the pure bubble hardening. In a 14Cr-YWTi nanostructured ferritic alloy with 12–14 at.% He implantation at 400 °C, the mean cavity size increased from 2.2 nm in the as-implanted case to 2.7 nm after the PIA at 750 °C/100 h [15]. The corresponding number densities of cavities increased from $\sim 8 \times 10^{23}$ m^{-3} to $\sim 12 \times 10^{23}$ m^{-3} after the PIA [16]. Nevertheless, hardening was not addressed in those works [15,16].

Therefore, in this study, at first, we aimed to investigate the effect of high concentration He implantation at various temperatures. Second, the post-implantation annealing behavior of NI hardness and the microstructure evolution process were examined to assess the contribution of cavities to the hardening.

2. Material and methods

The material used in this study was a 15Cr-ODS ferritic steel which was produced by mechanical alloy processing, followed by hot extrusion and forging at 1150 °C. The final heat treatment was an annealing at 1150 °C for 1 h followed by air-cooling. The resultant compositions (wt.%) were Fe-14.59Cr-1.84W-0.14Ti-3.46Al-0.27Zr-0.33Y_2O_3. The averaged grain size of the studied ODS steel was estimated to be about 370 nm based on electron backscatter diffraction (EBSD) measurements [12].

Specimens were sampled so that the specimen surface was perpendicular to the extrusion direction. The specimen surface was mechanically polished and then electrolytic polishing was conducted in a solution of 10% (vol.) $HClO_4$ and 90% (vol.) CH_3COOH at room temperature. Specimens were irradiated with 1 MeV He^+ at the DuET facility in Kyoto University [17]. The beams were by the raster scan at a frequency of 1000 Hz in a horizontal direction and 300 Hz in a vertical direction. He^+ beam was inclined with 45° to the normal of the specimen surface and a rotating energy degrader foil was applied for obtaining a rather homogenous distribution of helium atoms in the specimens. The averaged flux of He^+ ions was 1.7×10^{16} ions m^{-2} s^{-1}. The irradiation temperature was measured by an infrared thermography to be 300, 550 and 700 °C with in a fluctuation of ± 10 °C. The injected helium concentration and displacement damage (displacements per atom, dpa) were obtained by SRIM [18] simulation with use of the Kinchin-Pease method (shown in Fig. 1), recommended by Stoller et al. [19]. At the region 1000–1300 nm from the specimen surface, the He concentration was about 3500 appm and the corresponding damage level was approximately 0.2 dpa.

Specimens as implanted at 300 °C, which were placed in one evacuated quartz tube with Zr thin films for mitigating the surface oxidation of the specimens, were annealed at 800 °C for 100 h in a vacuum of 6×10^{-3} Pa followed by furnace-cooling. In order to eliminate the effect of aging itself, as-received specimens were also aged at 800 °C for 100 h and compared with those He-implanted specimens.

Cross-sectional transmission electron microscopy (TEM) specimens were fabricated by the lift-out technique using a Focused Ion Beam (FIB). Prior to TEM observations, flash polishing was done by using a solution of 5% (vol.) $HClO_4$ and 95% (vol.) CH_3OH at approximately

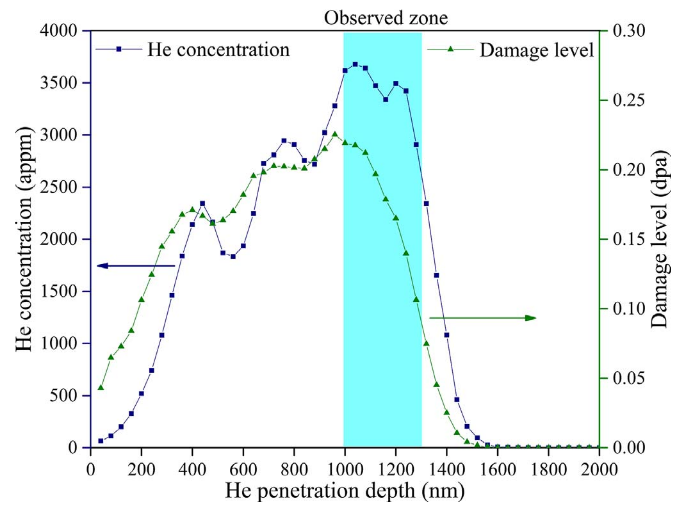

Fig. 1. He concentration (appm) and damage level (dpa) of a Fe-15Cr alloy as a function of the He-ion penetration depth, as predicted by SRIM simulation (He implanted to a fluence of 4.5×10^{20} He m^{-2}).

−35 °C for the removal of FIB damage layer. Subsequently, the microstructure was observed by using a conventional 200 kV JEOL JEM 2010 microscope. Further, cavities were imaged by the Fresnel contrast and the cavity size was carefully measured one by one according to the edge dark fringe (under-focus) or bright fringe (over-focus) of cavities. More details were described in the Ref. [12].

Nanoindentation (NI) tests were carried out by using a nanoindenter (Agilent G200) equipped with a Berkovich tip at 20 °C. Continuous stiffness measurement (CSM) was adopted to obtain the profiles of continuous hardness and elastic modulus versus indentation displacement. Before testing, the indenter tip geometry was calibrated by indenting a standard material fused silica. Key testing parameters were as follows: the strain rate was 0.05 s^{-1}, the harmonic displacement was 1 nm and the testing Poisson's ratio of ODS samples was 0.3. For each specimen, 24 testing points (50 µm between two adjacent points) were chosen and the averaged hardness was obtained by calculating the measured hardness data of roughly 20 tests.

3. Results and discussion

3.1. He-ion implantation hardening

The depth profiles of the averaged nanoindentation hardness (H_{NI}) for the as-received and as-implanted specimens are shown in Fig. 2(a), indicating that the averaged H_{NI} continuously decreased with increasing the indentation depth (h) from roughly 50 nm to 1500 nm, which is known as the indentation size effect (ISE) [20]. In order to evaluate irradiation hardening, we needed to choose an adequate depth that reflects microstructural changes by ion implantation. The hardness in the near surface depth region, which is shallower than 200 nm, is strongly affected by the depth because of the ISE, whereas in the region deeper than 300 nm, the hardness may already be influenced by unirradiated region since the depth of the plastic deformation region created by a nanoindent is approximately five times or more of the indentation depth [21–24]. Therefore, we selected the indentation depth of 250 nm as a reference H_{NI} to evaluate He-implantation hardening [23,24]. All the depth profiles in Fig. 2(a) show the similar trend. The profiles of He-implanted specimens at 300 and 550 °C are located at the upper side but that at 700 °C is at the lower side of as-received specimen, although the differences are within an error bar.

Nix and Gao developed a model to evaluate a bulk relevant macrohardness for a surface thin layer based on the concept of geometrically necessary dislocations [20], which is described in the following